Experimental determination of added hydrodynamic resistance caused by marine biofouling on ships

Osman Turan*, Yigit Kemal Demirel, Sandy Day and Tahsin Tezdogan

Department of Naval Architecture, Ocean and Marine Engineering, University of Strathclyde
100 Montrose Street, Glasgow, G4 0LZ, United Kingdom

Abstract

An extensive series of towing tests using flat plates covered with artificial barnacles were carried out at the Kelvin Hydrodynamics Laboratory (KHL) at the University of Strathclyde. The tests were designed to examine the effect of the coverage percentage of barnacles on the resistance and effective power of ships, over a range of Reynolds numbers.
This paper presents the added resistances due to calcareous fouling in terms of the added frictional resistance coefficient for a surface coverage of fouling of up to 20%, over different speeds (Reynolds numbers). The drag coefficients and roughness function values of each surface were evaluated. Roughness effects of the given fouling conditions on the frictional resistances of an LNG tanker were then predicted for different ship speeds using an in-house code which was developed based on the similarity law analysis of Granville (1958). Added resistance diagrams were then plotted using these predictions. Finally, powering penalties of the LNG tanker were predicted using the generated diagrams.

Keywords: Artificial barnacles; experiment; added resistance; biofouling

1. Introduction

Roughness of a ship's hull, which is often caused by marine coatings and biofouling, can dramatically increase a ship's frictional resistance and hence its fuel consumption and greenhouse gas emissions. Although a large body of research has been devoted to assess the effects of fouling on ship resistance and powering, little effort has been made to classify fouling conditions and relate them to full-scale ship frictional resistance.

Experimental, lab-scale studies provide reliable data since the uncertainties can be estimated to a degree. Therefore, several experimental studies have been devoted towards investigating the roughness effect on the skin friction. The very first experimental investigation into the effect of hull roughness on frictional resistance can be attributed to Froude (1872, 1874). According to Woods Hole Oceanographic Institution (1952), McEntee (1915) conducted the first extensive experimental study investigating the effect of fouling on frictional resistance. Flat plates were coated with anti-corrosive paints and kept in water for a given period of time. The plates were then towed with barnacles on them. The findings were remarkable since the resistance of the plates after 12 months of sea exposure increased to 4 times the resistance of an otherwise identical clean plate (Woods Hole Oceanographic Institution, 1952). As reported by Townsin (2003), Kempf (1937) conducted tests on pontoons covered with shell fouling and recorded an increase of 66% in the resistance, even with only 5% coverage. According to Schultz and Swain (2000), the increase in the frictional resistances of surfaces covered with slime was surveyed by conducting towing tests of flat plates by Benson et al. (1938), and performing experiments on cylinders, rotating disks and a model ship by Watanabe et al. (1969). Lewkowicz and Das (1986) conducted towing tests of flat plates covered with artificial slime and the increase in the frictional resistance due to artificial slime was found to be 18% (Schultz and Swain, 2000). Loeb et al. (1984) conducted rotating disk experiments using disks covered with several different types of microbial slimes. It was observed that microbial slime led to an increase of 10% to 20% in the frictional

* Corresponding author. Tel.: +44 (0)141 5483211; fax: +44 (0)141 5522879.
E-mail address: o.turan@strath.ac.uk

resistance. Schultz and Swain (1999) and Schultz (2000) investigated the effects of biofilms and algae on the skin friction coefficients of flat plates using boundary layer measurements. Swain et al. (2007) surveyed the fouling growth on different types of coatings under static and dynamic conditions. Andrewartha et al. (2010) measured an increase of 99% in the drag coefficients of test plates due to biofilms in a recirculating water tunnel. These findings clearly demonstrate that the antifouling and hydrodynamic performances of coatings vary significantly depending upon operational conditions. Although these experimental studies presented reliable information, they do not necessarily present a well-defined parametric study in order to deeply understand the effect of barnacle coverage on the frictional resistance of a ship. A means of assessing the effect of the coverage percentage of barnacles on ship resistance and powering would therefore be of great benefit.

With the aim of developing a scientific and fundamentally sound approach for predicting the effect of biofouling on added resistance, and hence the increase in power requirements, this paper presents a novel experimental approach towards establishing a method to predict the added resistance caused by calcareous fouling.

Actual barnacles of differing sizes, which represent time based fouling, were scanned in 3D in order to model the barnacles in a digital environment. The digital models of the barnacles were then printed in 3D using 3D printing technology to generate artificial barnacles. The artificial barnacles were glued onto the surface of the flat plates and then towing tests of the flat plates were conducted at various speeds. The roughness functions and roughness Reynolds number were then evaluated using the overall method of Granville (1987) using the present experimental data.

This technique provides a unique opportunity to systematically determine the effects of different levels of fouling coverage on the hydrodynamic resistance of plates. This systematic approach also eliminates the problems and uncertainties which are encountered during the transportation of the immersed plates from the sea to the tank, including the transfer of the marine life from seawater to freshwater.

3 different coverage percentages, with even distributions, and 1 bare plate, which serves as a reference plate, are considered in the experiments as given below:

- Reference Plate (Bare Plate)
- 5%
- 10%
- 20%

A well-known similarity law scaling procedure from Granville (1958) can be used to predict the effect of such roughness on the frictional resistance of flat plates of ship lengths, provided that the roughness function behaviour of such fouling is known (Schultz, 2007). Some examples of the use of this method are given by Schultz (2002), Schultz (2004), Shapiro (2004), Schultz (2007), Flack and Schultz (2010) and Schultz et al. (2011). Schultz (2007) proposed a methodology to predict the effects of a range of coating and biofouling conditions on ship frictional resistance, using his experimental data, by means of the similarity law scaling procedure of Granville (1958). However, it may be difficult for less experienced users to carry out such an analysis using this methodology. Goal-based, simple added resistance diagrams for predicting the effect of biofouling on ship frictional resistance would therefore be of great benefit.

One of the aims of the present paper is therefore to generate such diagrams using an in-house code based on the similarity law scaling procedure explained by Schultz (2007), for a given set of fouling conditions. The proposed diagram enables the prediction of the added frictional resistance coefficients of an LNG carrier of 270 m due to the given fouling coverage on her hull for a range of ship speeds. The predictions of the increase in the effective power of the LNG carrier were made using the diagram.

This paper is organised as follows: Experimental facilities and model details are explained in detail in Section 2 while the methodology followed within the paper is presented in Section 3. In Section 4, the frictional resistance coefficients and roughness functions of the test surfaces are demonstrated and an added resistance diagram is plotted. In addition, powering predictions of the LNG carrier are made using the generated diagrams. Finally, the results of the study are discussed in Section 5, along with recommendations for future avenues of research.

2. Experimental facilities and model details

The experiments were carried out at the Kelvin Hydrodynamics Laboratory (KHL) of the University of Strathclyde. The KHL test tank has dimensions of 76.0 m x 4.6 m x 2.5 m. The tank is equipped with a digitally-controlled towing carriage, state-of-the-art absorbing wavemaker, and a highly effective sloping beach. The carriage has a velocity range of 0 – 5 m/s, with the velocity range used in these experiments kept between 1.5 and 3.6 m/s. Fresh water was used in the experiments. The temperature of the water was monitored during the experiments in order to be able to evaluate drag coefficients according to the temperature.

The flat plates used for the tests were manufactured from 304 stainless steel grade sheet stock. Fig. 1 depicts the dimensions of the flat plates. The leading edges of the plates were shaped to a radius of 2.5 mm while the trailing edge was kept sharp in order to mitigate the extra drag due to the separation as much as possible. The flatness of the plates, as well as their dimensions, were checked using a CNC machine.

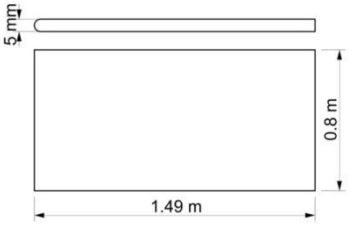

Fig. 1. Dimensions of the flat plates.

The artificial barnacles used in the experiments were 3D printed using 3D scans of real barnacles. The real barnacles were bought and scanned using a 3D scanner system. Individual barnacle models were created using the 3D scans of these barnacles. The most appropriate one, which corresponds to the real barnacles seen on ship hulls, was selected among them.

The selected model was then scaled based on the typical dimensions of the barnacles seen on ship hulls. Different sizes of barnacles were manufactured based on observations from ship hulls, as well as based on the studies of Larsson et al. (2010) and Schultz (2004). A very large juvenile, measuring 5 mm high, was chosen to be the working barnacle sample.

The Reference Plate was the plate which the artificial barnacles were glued onto with 5%, 10% and 20% coverage. Therefore, firstly the Reference Plate was towed in the tank when it was bare, in order to obtain the baseline for the other configurations. Following the completion of the tests for this initially bare Reference Plate, the plate was removed from the water and barnacles were glued on to achieve 5% coverage. The plate was then then put back into the water for the tests. The same procedure was repeated for 10% and 20% surface coverage. It is of note that the distribution pattern applied to the Reference Plate 1 followed the recommendations of ASTM-D6990-05 (2011).

Both sides of Plate 1 were covered with barnacles such that they covered 5% of each wetted surface area and Plate 2 was covered with barnacles such that they covered 10% of each wetted surface area. Plate 3 was covered with barnacles such that they covered 20% of each wetted surface area. Fig. 2 shows the Reference Plate and Plate 1, whereas **Error! Reference source not found.** shows Plate 2 and Plate 3.

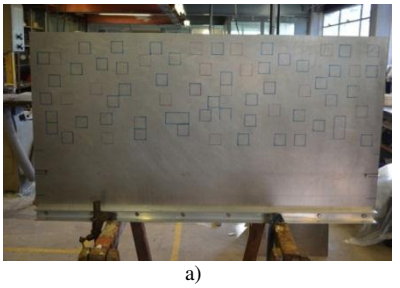

a)

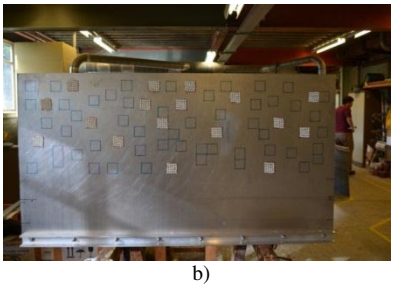

b)

Fig. 2. (a) Reference Plate; (b) Plate 1.

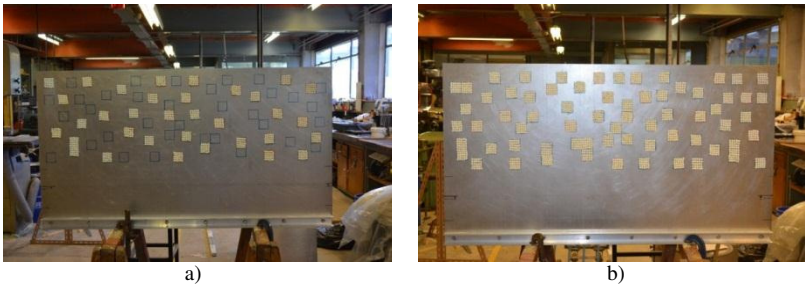

a) b)

Fig. 3. (a) Plate 2; (b) Plate 3.

3. Methodology

The total resistance (drag) of a flat plate, R_T, is mainly composed of two components; the residuary resistance, R_R, and the frictional resistance, R_F, as given by (1).

$$R_T = R_R + R_F \tag{1}$$

Once the total drag, R_T, values were obtained for each plate and related speeds, they were non-dimensionalised by dividing each term by the dynamic pressure and wetted surface area of the plates. The total drag coefficient, C_T, was therefore evaluated using the following equation (2)

$$R_T = \frac{1}{2}\rho S C_T V^2 \tag{2}$$

where ρ is the density of water, S is the wetted surface area, C_T is the total resistance coefficient and V is the speed.

Showing similarity to the resistance decomposition, the total resistance coefficient, C_T, is made up of the residuary resistance coefficient, C_R, and the frictional resistance coefficient, C_F. Given that the residuary resistance coefficient is a function of the Froude number, Fr, and the frictional resistance coefficient is a function of the Reynolds number, Re, the total resistance coefficient can, therefore, be written in the following form (Schultz, 2007):

$$C_T = C_R(Fr) + C_F(Re) \tag{3}$$

The Karman-Schoenherr friction line (Schoenherr, 1932) given by (4) for a smooth plate can be used to predict the frictional resistance coefficients of a smooth flat plate. The C_F values of the reference smooth plate are therefore assumed to be equal to the C_F values obtained using (4). It is of note that Candries (2001) and Schultz (2004) also showed that equation (4) can be used for the prediction of the frictional resistance of flat plates.

$$\frac{0.242}{\sqrt{C_F}} = \log(Re \cdot C_F) \tag{4}$$

The differences between the C_T values obtained using the experimental data and the C_F values obtained using (4) were assumed to be the C_R values of the Reference Plate as shown by (5). The computed C_R values were taken to be

the C_R values of all the test surfaces (eq.(6)), since the residuary resistances of the plates were not expected to be significantly affected by the surface roughness (Schultz, 2007). Hence, the C_F values of the test surfaces were computed by subtracting the C_R values of the Reference Plate from the C_T values of the test surfaces as shown by (7). The mathematical process for this is outlined below.

$$C_{R_s} = C_{T_s} - C_{F_s} \tag{5}$$

$$C_{R_s} = C_{R_r} \tag{6}$$

$$C_{F_r} = C_{T_r} - C_{R_r} \tag{7}$$

Roughness Reynolds numbers, k^+, and roughness function values, ΔU^+, for all of the surfaces were obtained iteratively using (8) and (9) following the overall procedure of Granville (1987) using the present experimental data.

$$k^+ = \left(\frac{k}{L}\right)\left(\frac{R_{eL}C_F}{2}\right)\left(\sqrt{\frac{2}{C_F}}\right)_R\left[1-\frac{1}{\kappa}\left(\sqrt{\frac{C_F}{2}}\right)_R+\frac{1}{\kappa}\left(\frac{3}{2\kappa}-\Delta U^{+'}\right)\left(\frac{C_F}{2}\right)_R\right] \tag{8}$$

$$\Delta U^+ = \left(\sqrt{\frac{2}{C_F}}\right)_S - \left(\sqrt{\frac{2}{C_F}}\right)_R - 19.7\left[\left(\sqrt{\frac{C_F}{2}}\right)_S - \left(\sqrt{\frac{C_F}{2}}\right)_R\right] - \frac{1}{\kappa}\Delta U^{+'}\left(\sqrt{\frac{C_F}{2}}\right)_R \tag{9}$$

where L is the plate length, R_{eL} is the plate Reynolds number, C_F is the frictional drag coefficient, $\Delta U^{+'}$ is the roughness function slope, which is the slope of ΔU^+ as a function of ln(k+), and the subscript S indicates a smooth condition whereas the subscript R indicates a rough condition.

The prediction code was developed based on the similarity law scaling procedure of Granville (1958), which is explained in detail in Schultz (1998) and Schultz (2007). The evaluated k^+ and ΔU^+ values were then employed in the aforementioned code and predictions of the roughness effects of these particular fouling conditions on the frictional resistance of a flat plate representing an LNG carrier were made. The details of the procedure can be found in Demirel (2015). A graphical representation of the procedure is shown in Fig. 4.

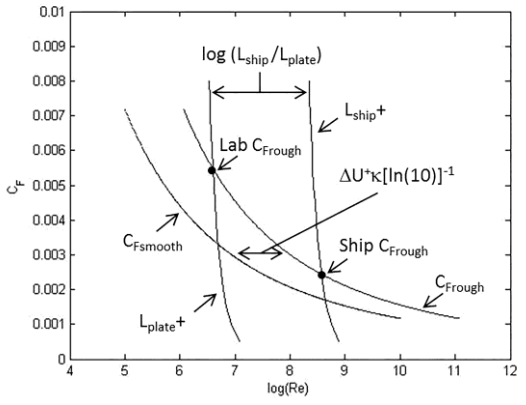

Fig. 4. Granville scale-up procedure (Demirel, 2015).

The increase in P_E due to the effect of fouling can be expressed by

$$\%\Delta P_E = \frac{C_{T,rough} - C_{T,smooth}}{C_{T,smooth}} \times 100 = \frac{\Delta C_F}{C_{T,smooth}} \times 100 \quad (10)$$

similar to that used by Tezdogan et al. (2015). ΔC_F is the added resistance coefficient due to surface roughness. $C_{T,smooth}$ on the other hand, includes other resistance components and the evaluation of this is not the subject of this study. The $C_{T,smooth}$ values of the LNG carrier were taken from the report of the experiments that were performed earlier at the Kelvin Hydrodynamics Laboratory at the University of Strathclyde.

4. Results

4.1. Frictional resistances and roughness functions

Fig. 5 illustrates the frictional resistance coefficients and Fig. 6 shows roughness functions of all of the test surfaces together with the roughness function model of Grigson (1992).

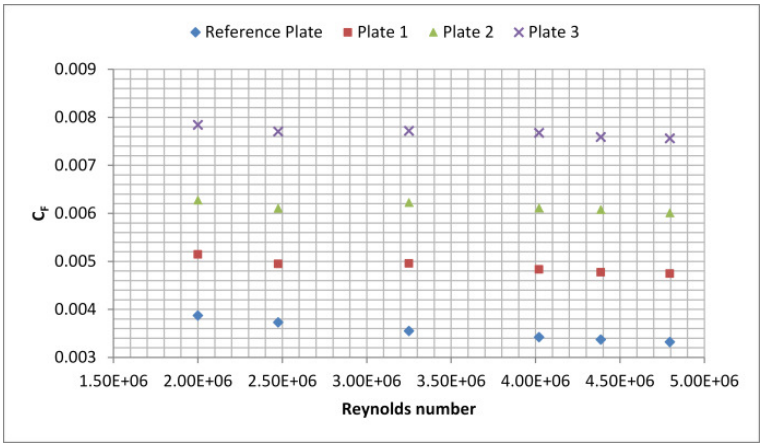

Fig. 5. Frictional resistance coefficients of all test surfaces.

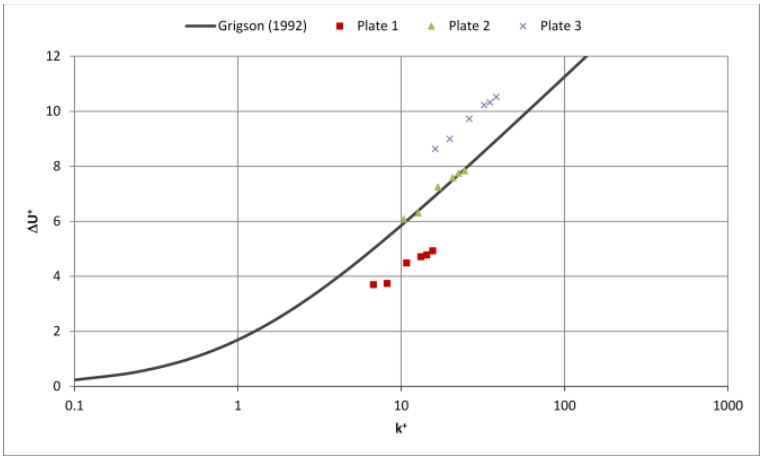

Fig. 6. The roughness functions for all of the test surfaces together with the roughness function model of Grigson (1992).

It is clearly seen in Fig. 5 that Plate 3, corresponding to 20% coverage, showed the highest drag characteristics among all of the surfaces, with an average increase of ~117% with respect to the Reference Plate. It is followed by Plate 2 and Plate 1 as expected, with average increases of ~74% and ~38%, respectively. The increases in C_F values ranged from ~33% to ~43% for Plate 1, from ~62% to ~81% for Plate 2, and from ~103% to ~128% for Plate 3, with respect to Reference Plate.

Shown for comparison in Fig. 6 is the Colebrook type roughness function model of Grigson (1992) together with the roughness functions of the test surfaces, using a logarithmic scale in the x-axis. It should be borne in mind that the roughness functions and roughness Reynolds numbers were calculated using $k=0.01h(\%coverage)^{1/2}$ as the roughness length scale, where h is the barnacle height. Using this scaling, a fairly good agreement was obtained between the roughness functions of Plate 2 and the roughness function model of Grigson (1992). As evident from Fig. 6, the roughness function behaviours of the test surfaces showed there was a monotonically increasing trend with the increasing roughness Reynolds numbers and that they reached the fully rough regime. Representative roughness function models can therefore be fitted to the roughness functions and the roughness functions at higher roughness Reynolds numbers can be extrapolated using the fitted equations.

Uncertainty estimates for the drag coefficients and roughness function calculations were made through repeatability tests using the procedure defined by the ITTC (2002). The repeatability tests were performed at two speeds, namely 1.857 m/s and 3.591 m/s, which correspond to Reynolds numbers of $\sim 2.6 \times 10^6$ and $\sim 5 \times 10^6$, respectively.

The bias uncertainty in C_F ranged from ±1.625% at the lower Reynolds number to ±0.368% at the higher Reynolds number, while the precision uncertainty in C_F ranged from ±0.743% at the lower Reynolds number to ±0.041% at the higher Reynolds number. The overall uncertainty in C_F ranged from ±1.787% at the lower Reynolds number to ±0.430% at the higher Reynolds number.

The overall uncertainty levels of the drag coefficients are satisfactory when compared to other experiments given in the literature such as Schultz (2004). The very small precision limits reveal the acceptable repeatability of the experiments.

4.2. Added resistance and effective power of an LNG carrier

The roughness functions and roughness Reynolds numbers given in the previous section were employed in the code and predictions of the added resistance coefficients, ΔC_F, were made for all fouling conditions. Predictions were made for a ship length of 270 m to represent an LNG carrier. The added resistance coefficients, ΔC_F, due to the given fouling conditions were plotted against several ship speeds. Logarithmic equations were then fitted to the ΔC_F values using the least squares method in order to evaluate added resistance diagrams (Fig. 8).

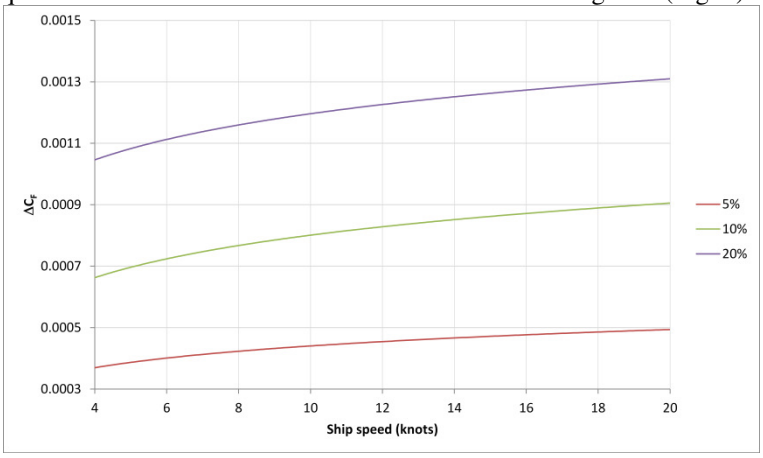

Fig. 7. Added resistance diagram for an LNG carrier with different fouling conditions.

Table 1 and Fig. 8 jointly illustrate the percentage increase in the frictional resistances and effective powers of the LNG carrier at 20 knots, calculated using the ΔC_F read from Fig. 7.

As can be seen from Table 1 and Fig. 8, the increases in the frictional resistance and effective power of the LNG carrier due to 5% barnacle coverage at design ship speed of 20 knots were predicted to be 36.8% and 22.5%, respectively. These values became 67.4% and 41.3% when calculating the increase in the frictional resistance coefficient, C_F, and effective power, P_E, due to 10% barnacle coverage. 20% barnacle coverage causes significant increases in C_F and P_E values, namely 97.5% and 59.7%, respectively.

Table 1. The increases in the frictional resistance and effective power of the LNG carrier at 20 knots.

Description of condition	% ΔC_F	% ΔP_E
Smooth	-	-
5%	36.8	22.5
10%	67.4	41.3
20%	97.5	59.7

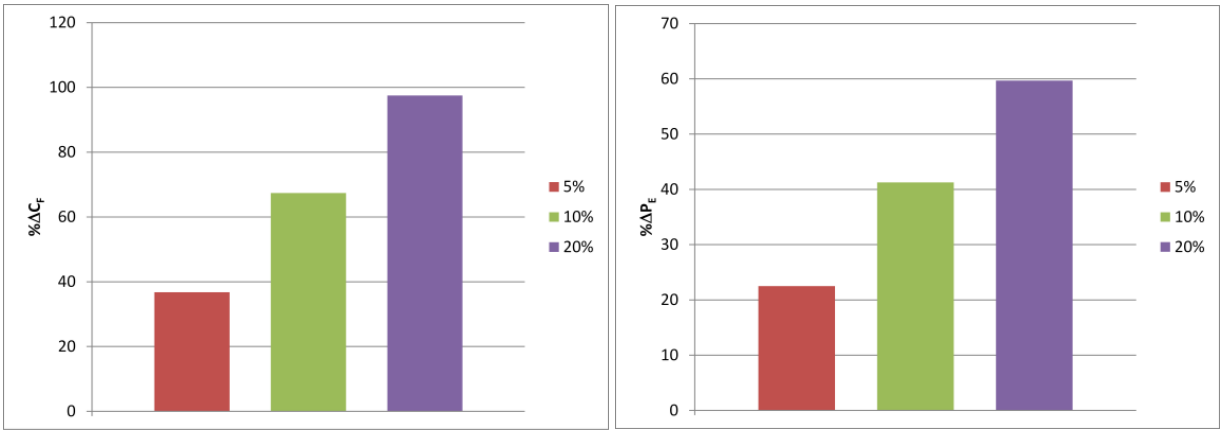

Fig. 8. (a) Percentage increase in (a) C_F values; (b) P_E values of the LNG carrier with respect to the smooth hull condition.

5. Discussion and Conclusions

An experimental study of the resistance of flat plates covered with artificial barnacles was made. Four flat plates having different surface conditions, including a smooth reference plate and three different surface coverages of barnacles were towed at the Kelvin Hydrodynamics Laboratory (KHL) of the University of Strathclyde.

The plates were towed at a range of speeds and the total resistances of the surfaces were measured. The resistance values were then non-dimensionalised. The frictional resistance coefficients of all of the test surfaces were then computed using assumptions that suggest the frictional resistance coefficients of smooth surfaces obey the Karman-Schoenherr friction line (Schoenherr, 1932) and that the residuary resistances of flat plates are not affected by surface roughness. Afterwards, roughness function values of all of the test surfaces were calculated using an indirect method, following the overall method of Granville (1987). Uncertainty estimates were made through repeatability tests, with the uncertainty values found to be sufficient to ensure a reliable comparison.

Following this, the obtained roughness functions and roughness Reynolds numbers were employed in an in-house code, developed based on the similarity law analysis of Granville (1958). The added frictional resistance coefficients of a flat plate representing an LNG carrier were then predicted for various ship speeds and an added resistance diagram was generated using these predictions. The increases in the effective power of the LNG carrier were then predicted for a ship speed of 20 knots using the added resistance diagram.

The diagram has a key advantage in that it captures the complex hydrodynamic response of fouling in simple curves which can be implemented in a spreadsheet or a tool for life-cycle cost estimation. The main advantage of the proposed diagram is that it directly enables the use of surface conditions, ship length and ship speed, rather than having to use hydrodynamic parameters. By using such diagrams, one can easily estimate the added resistance, and hence the fuel penalty, of a ship for a particular fouling condition given in this study. Therefore it becomes very practical to calculate the effect of a range of fouling conditions on frictional resistance.

It is of note that this approach assumes a homogenous distribution of fouling on flat plates of ship hulls, which may not necessarily be the case on real ship hulls. Therefore, additional results from further immersion tests and experiments considering different types of fouling and their spatial distributions would be beneficial to improve the diagrams. Having said that, the present diagrams may be considered as a leap forward towards a universal model.

This paper not only proposes diagrams but it also provides the algorithm of a prediction procedure showing how to develop such diagrams using the available experimental data.

A future work might be to test different sizes of barnacles and other types of fouling, and then obtain new roughness function models and generate new added resistance diagrams for the tested surfaces.

Acknowledgements

The authors gratefully acknowledge that the research presented in this paper was partially generated as part of the EU funded FP7 project FOUL-X-SPEL (Environmentally Friendly Antifouling Technology to Optimise the Energy Efficiency of Ships, Project number 285552, FP7-SST-2011-RTD-1).

References

Andrewartha, J., Perkins, K., Sargison, J., Osborn, J., Walker, G., Henderson, A. & Hallegraeff, G. 2010. Drag force and surface roughness measurements on freshwater biofouled surfaces. Biofouling, 26, 487-496.

ASTM-D6990-05 2011. Standard Practice for Evaluating Biofouling Resistance and Physical Performance of Marine Coating Systems.

Benson, J., Ebert, J. & Beery, T. 1938. Investigation in the NACA tank of the effect of immersion in salt water on the resistance of plates coated with different shipbottom paints. NACA Memorandum Report C&R C-S19-1(3).

Candries, M. 2001. Drag, boundary-layer and roughness characteristics of marine surfaces coated with antifoulings. PhD Thesis, University of Newcastle upon Tyne.

Demirel, Y. K. 2015. Modelling the roughness effects of marine coatings and biofouling on ship frictional resistance. PhD Thesis, University of Strathclyde.

Flack, K. A. & Schultz, M. P. 2010. Review of Hydraulic Roughness Scales in the Fully Rough Regime. Journal of Fluids Engineering, 132, 041203-041203.

Froude, W. 1872. Experiments on the surface-friction experienced by a plane moving through water. British Association for the Advancement of Science. The Collected Papers of William Froude, Institution of Naval Architects, 1955.

Froude, W. 1874. Report to the Lords Commissioners of the Admiralty on Experiments for the Determination of the Frictional Resistance of Water on a Surface, Under Various Conditions, Performed at Chelston Cross, Under the Authority of Their Lordships, 44th Report by the British Association for the Advancement of Science.

Granville, P. S. 1958. The frictional resistance and turbulent boundary layer of rough surfaces. Journal of Ship Research, 2, 52-74.

Granville, P. S. 1987. Three indirect methods for the drag characterization of arbitrarily rough surfaces on flat plates. Journal of Ship Research, 31, 70-77.

Grigson, C. 1992. Drag losses of new ships caused by hull finish. Journal of Ship Research, 36, 182-196.

ITTC 2002. Uncertainty Analysis, Example for Resistance Test. ITTC Recommended Procedures and Guidelines, Procedure 7.5-02-02-02, Revision 01.

Kempf, G. 1937. On the effect of roughness on the resistance of ships. Trans INA, 79, 109-119.

Larsson, A. I., Mattsson-Thorngren, L., Granhag, L. M. & Berglin, M. 2010. Fouling-release of barnacles from a

boat hull with comparison to laboratory data of attachment strength. Journal of Experimental Marine Biology and Ecology, 392, 107-114.

Lewkowicz, A. & Das, D. 1986. Turbulent boundary layers on rough surfaces with and without a pliable overlayer: a simulation of marine fouling. International Shipbuilding Progress, 33, 174-186.

Loeb, G., Laster, D. & Gracik, T. 1984. The influence of microbial fouling films on hydrodynamic drag of rotating discs. In: COSTLOW, J. D. & TIPPER, R. (eds.) Marine Biodeterioration: An Interdisciplinary Study. Naval Institute Press, Annapolis, MD.

McEntee, W. 1915. Variation of frictional resistance of ships with condition of wetted surface. Trans. Soc. Nav. Arch. Mar. Eng., 24, 37-42.

Schoenherr, K. E. 1932. Resistances of flat surfaces moving through a fluid. Transactions of SNAME, 40, 279-313.

Schultz, M. P. 1998. The Effect of Biofilms on Turbulent Boundary Layer Structure. PhD Thesis, Florida Institute of Technology.

Schultz, M. P. 2002. The relationship between frictional resistance and roughness for surfaces smoothed by sanding. Journal of Fluids Engineering, 124, 492-499.

Schultz, M. P. 2004. Frictional resistance of antifouling coating systems. Journal of Fluids Engineering, 126, 1039-1047.

Schultz, M. P. 2007. Effects of coating roughness and biofouling on ship resistance and powering. Biofouling, 23, 331-341.

Schultz, M. P., Bendick, J. A., Holm, E. R. & Hertel, W. M. 2011. Economic impact of biofouling on a naval surface ship. Biofouling, 27, 87-98.

Schultz, M. P. & Swain, G. 1999. The effect of biofilms on turbulent boundary layers. Journal of Fluids Engineering, 121, 44-51.

Schultz, M. P. & Swain, G. W. 2000. The influence of biofilms on skin friction drag. Biofouling, 15, 129-139.

Shapiro, T. A. 2004. The effect of surface roughness on hydrodynamic drag and turbulence. USNA Trident Scholar Project Report No. 327.

Swain, G. W., Kovach, B., Touzot, A., Casse, F. & Kavanagh, C. J. 2007. Measuring the Performance of Today's Antifouling Coatings. Journal of Ship Production, 23, 164-170.

Tezdogan, T., Demirel, Y. K., Kellett, P., Khorasanchi, M., Incecik, A. & Turan, O. 2015. Full-scale unsteady RANS CFD simulations of ship behaviour and performance in head seas due to slow steaming. Ocean Engineering, 97, 186-206.

Townsin, R. L. 2003. The Ship Hull Fouling Penalty. Biofouling, 19, 9-15.

Watanabe, S., Nagamatsu, N., Yokoo, K. & Kawakami, Y. 1969. The augmentation in frictional resistance due to slime. J. Kansai Soc. Nav. Arc., 131, 45-51.

Woods Hole Oceanographic Institution 1952. Marine Fouling and Its Prevention, Annapolis, Maryland, United States Naval Institute.